Waveguides Induced by Closed-circuit Gray Photovoltaic Solitons*

CHEN Dan[1], ZHANG Mei-zhi[2,3], YANG Yan-long[3], LU Ke-qing[3]

(1 *State Key Laboratory of Integrated Service Networks, Xidian University, Xi'an* 710071, *China*)
(2 *School of Electronics Engineering, Xi'an University of Post and Telecommunication, Xi'an* 710061, *China*)
(3 *State Key Laboratory of Transient Optics and Photonics, Xi'an Institute of Optics and Precision Mechanics, Chinese Academic of Sciences, Xi'an* 710119, *China*)

Abstract: The theory of waveguides induced by gray solitons in closed-circuit photovoltaic crystals is analyzed. The study shows that waveguides induced by gray closed-circuit photovoltaic solitons are only a single guided mode for all soliton graynesses and all values of both the electric current density and the ratio between the soliton peak intensity and the dark irradiance. The results explain that the confined energy near the center of a gray closed-circuit photovoltaic soliton increases with the electric current density and decreases with an increase in both the soliton grayness and ratio between the soliton peak intensity and dark irradiance. Relevant examples are provided where the photovoltaic crystal is assumed to be $LiNbO_3$.

Key words: Soliton waveguide; Photorefractive effect; Nonlinear optics

CLCN: O437.5 **Document Code**: A **Article ID**: 1004-4213(2009)12-3145-5

0 Introduction

Photorefractive (PR) spatial solitons have attracted a great deal of attention in the last decade[1-17]. It is now well established that they form at very low power levels (microwatt and lower) and are stable in both (1+1) and (2+1) dimensions. Therefore, such PR solitons are considered to be among the prime candidates for the building blocks of all-optical switching devices where light itself guides and steers light without fabricated waveguides. Among the numerous types of photorefractive soliton, the most commonly used type is photorefractive steady-state spatial solitons, i. e., screening solitons[5-6] and photovoltaic (PV) solitons[7-8]. Recently, steady-state screening-photovoltaic solitons have been predicted[9] and observed[10] in biased photorefractive- photovoltaic crystals, which change into screening solitons when the bulk PV effect is neglected and PV solitons when the external bias field is absent. Thus far, bright, dark, and gray steady-state soliton domains have been predicted. Of particular interest are waveguides induced by photorefractive solitons, which can be used in various waveguide applications and in multiple configurations, such as directional couplers[11], beam splitters (Y junctions)[12], and nonlinear frequency conversion[13]. Recent theoretical and experimental work have shown waveguides induced by bright and dark screening solitons[14], by bright and dark photovoltaic solitons[15-16], and by bright and dark screening- photovoltaic solitons[17]. However, can a gray soliton in a closed-circuit photovoltaic crystal induce a waveguide? This intriguing and challenging question has not been investigated yet.

In this paper, we show the theory of waveguides induced by gray solitons in closed-circuit photovoltaic crystals, which exhibits that waveguides induced by gray closed-circuit photovoltaic solitons are only a single guided mode for all soliton graynesses and all values of both the electric current density and the ratio between the soliton peak intensity and the dark irradiance. Our analysis indicates that the confined energy near the center of a gray closed-circuit photovoltaic soliton increases with the electric current density and decreases with an increase in both the soliton grayness and the ratio between the soliton peak intensity and the dark irradiance. Relevant examples are provided where the photovoltaic crystal is assumed to be $LiNbO_3$.

1 Theory and analysis

To start, let us consider an optical beam that propagates in a photovoltaic material along the z axis and is allowed to diffract only along the x direction. For the convenience of the analysis, let the photovoltaic material is $LiNbO_3$ with its optical c-axis oriented along the x coordinate. In this

*Supported by the National Natural Science Foundation of China (10674176)
Tel: 029-88202529-806 Email: dan_chen@tom.com
Received date: 2008-09-28 Revised date: 2009-01-19

case, the crystal's refractive index perturbation is given by[8] $\Delta n_e = -0.5 n_e^3 r_{33} E_{sc}$, where n_e is the unperturbed extraordinary index of refraction, r_{33} is the electro-optic coefficient, and E_{sc} is the space-charge field induced in this photovoltaic material. In paraxial approximation case, the expression for the refractive index perturbation, $\Delta n_e = -0.5 n_e^3 r_{33} E_{sc}$, leads to $n_e'^2 = n_e^2 - n_e^4 r_{33} E_{sc}$, where n_e' is the perturbed extraordinary refractive index (along the c-axis). On the other hand, the electric-field component E of the optical beam satisfies the Helmholtz equation

$$\nabla^2 E + (k_0 n_e')^2 E = 0 \tag{1}$$

where $k_0 = 2\pi/\lambda_0$ is the free-space wave vector and λ_0 is the common free-space wavelength. By expressing E in terms of slowly varying envelope φ, i.e., $E = i\varphi(x,z)\exp(ikz)$, where $k = k_0 n_e$ is the propagation constant, we find that Eq. (1) leads to the following evolution equation

$$i\varphi_z + \frac{1}{2k}\varphi_{xx} - \frac{k_0 (n_e^3 r_{33} E_{sc})}{2}\varphi = 0 \tag{2}$$

where $\varphi_z = \partial\varphi/\partial z$, etc.

The space-charge field E_{sc} can then be obtained from the transport model of Kukhtarev et al. Under steady-state conditions and for typical photovoltaic crystals, the space-charge field E_{sc} is approximately given by[8]

$$E_{sc}(x) = E_p \frac{J - I(x)}{I(x) + I_d} \tag{3}$$

where $E_p = \kappa\gamma_e N_A/e\mu$ is the photovoltaic field constant, N_A is the density of negatively charged acceptors, κ is the photovoltaic constant, μ is the electron mobility, γ_e is the recombination rate coefficient, e is the electron charge, $J = \hat{J}/\hat{s}\kappa N_d$, $\hat{J}$ is the electric current density, N_d is the total donor density, $\hat{s}$ is the photoexcitation cross section, I is the power density of the optical beam, and I_d is the so-called dark irradiance. Note that J can vary continuously from zero (at $R \to \infty$) to the maximum value of J (at $R \to 0$), where R is the external resistance[8]. Moreover, the beam power density I can be expressed in terms of the envelope φ by use of Poynting's theorem, i.e., $I = (n_e/2\eta_0)|\varphi|^2$, where $\eta_0 = (\mu_0/\varepsilon_0)^{1/2}$ is the vacuum intrinsic impedance. For simplicity, let us adopt the following dimensionless coordinates and variables: $\xi = z/(kx_0^2)$, $s = x/x_0$, and $\varphi = (2\eta_0 I_d/n_e)^{1/2} U$, where x_0 is an arbitrary spatial width. By employing these latter transformations and by substituting Eq. (3) into Eq. (2), we find that the normalized envelope U obeys the following dynamical evolution equation

$$iU_\xi + \frac{1}{2}U_{ss} - \delta\frac{(J - |U|^2)U}{1 + |U|^2} = 0 \tag{4}$$

where $\delta = (k_0 x_0)^2 (n_e^4 r_{33}/2) E_p$. To find the gray photovoltaic soliton solutions of Eq. (4), let us express the normalized envelope U in the following fashion[6]

$$U = \rho^{1/2}\phi(s)\exp\left[i\left(\nu\xi + \int_0^s \frac{\Gamma ds'}{\phi^2(s')}\right)\right] \tag{5}$$

where Γ is a real constant to be determined, ν is a nonlinear shift of the propagation constant, and $\phi(s)$ is a normalized function bounded between $0 \leqslant \phi(s) \leqslant 1$. The positive quantity ρ is defined as $\rho = I_\infty/I_d$, where $I_\infty = I(x \to \pm\infty, z)$. By substituting Eq. (5) into Eq. (4), we find that the normalized function $\phi(s)$ satisfies the following ordinary differential equation

$$\varphi'' - 2\nu\varphi - \frac{\Gamma^2}{\varphi^3} - 2\delta\frac{(J - \rho\varphi^2)\varphi}{1 + \rho\varphi^2} = 0 \tag{6}$$

where $\phi'' = d^2\varphi/ds^2$, etc. Moreover, when $\rho << 1000$, the maximum value of J is given by $J_{max} \approx \rho$[8]. For a gray soliton the boundary conditions are $\phi(0) = \sqrt{m}$ $(0 < m < 1)$, $\phi(s \to \pm\infty) = 1$, $\phi'(0) = 0$, and $\phi'(s \to \pm\infty) = \phi''(s \to \pm\infty) = 0$. The m parameter describes the soliton grayness, i.e., the intensity at the middle of the wave defined as $I(0) = mI_\infty$. Substituting $s \to \infty$ and the boundary conditions $\phi(s \to \infty) = 1$ and $\phi''(s \to \infty) = 0$ into Eq. (6) leads to

$$\Gamma^2 = -2[\nu + \delta(J - \rho)/(\rho + 1)] \tag{7}$$

By integrating Eq. (6) and by employing $\phi(s \to \infty) = 1$, $\phi'(s \to \infty) = 0$, $\phi'(0) = 0$, and $\phi^2(0) = m$, we find that

$$\nu = \frac{\delta m}{m - 1} - \frac{\delta}{(m-1)^2}\left[\frac{(J - \rho)(1 - m)}{\rho + 1} + m\left(1 + \frac{J - \rho}{\rho + 1}\right)\frac{\rho + 1}{\rho}\ln\left(\frac{1 + \rho m}{1 + \rho}\right)\right] \tag{8}$$

$$(\phi')^2 = 2(\nu - \delta)(\phi^2 - 1) + 2\left[\nu + \frac{\delta(J - \rho)}{\rho + 1}\right]\left(\frac{1 - \phi^2}{\phi^2}\right) + 2\delta\left(1 + \frac{J - \rho}{\rho + 1}\right)\frac{\rho + 1}{\rho}\ln\left(\frac{1 + \rho\phi^2}{1 + \rho}\right) \tag{9}$$

from which the gray envelope $\phi(s)$ can be determined by numerical integration. Note that the set of parameters J, δ, ρ, and m has to be judiciously selected so that $(\phi')^2 > 0$ and $\Gamma^2 > 0$. After the steady-state gray photovoltaic soliton has formed, the space-charge field E_{sc} is present in the photovoltaic material, and thus the refractive index gives rise to a change. At this point, let us consider a probe beam propagating in this soliton-induced waveguide. The optical field $\bar{E}_{opt}$ of the probe beam is then expressed in terms of a slowly

varying envelope ψ, i. e., $\bar{E}_{opt}(x,z,t)=\psi(x)\exp(i\bar{\beta}z-i\bar{\omega}t)$, where $\bar{\beta}$ is the propagation constant and $\bar{\omega}$ is the frequency of the probe beam. In this case and from the Helmholtz equation, the wave equation can be readily obtained and it is given by

$$\frac{d^2\psi}{dx^2}+[\bar{k}_0^2\bar{n}^2(x)-\bar{\beta}^2]\psi=0 \tag{10}$$

where

$$\bar{n}(x)=\bar{n}_e+\Delta\bar{n}(x)=\bar{n}_e-\frac{1}{2}\bar{n}_e^3\bar{r}_{33}E_{sc} \tag{11}$$

$\bar{k}_0=2\pi/\bar{\lambda}_0$ is the wave vector in vacuum, and $\bar{\lambda}_0$ is the common free-space wavelength used. Note that the values of unperturbed refractive index $\bar{n}_e$ and the electro-optic coefficient $\bar{r}_{33}$ are now subject to the new wavelength $\bar{\lambda}_0$. Under paraxial approximation conditions Eq. (11) leads to $\bar{n}^2=\bar{n}_e^2-\bar{n}_e^4\bar{r}_{33}E_{sc}$. Substituting the expression we have just found for $\bar{n}^2$ into Eq. (10) leads to

$$\frac{d^2\psi}{d\bar{s}^2}=\left\{\bar{\tau}+\frac{\delta\left[J-\rho\varphi^2\left(\frac{\bar{s}}{\sqrt{2}\sigma_1\sigma_2}\right)\right]}{1+\rho\varphi^2\left(\frac{\bar{s}}{\sqrt{2}\sigma_1\sigma_2}\right)}\right\}\psi \tag{12}$$

where the normalized propagation constant $\bar{\tau}$, the new normalized length $\bar{s}$, and normalization factors σ_1 and σ_2 are respectively defined as

$$\bar{\tau}=\frac{\bar{\beta}^2-\sigma_1^2k^2}{2\sigma_1^2\sigma_2^2/x_0} \tag{13}$$

$$\bar{s}=\sqrt{2}\sigma_1\sigma_2 s \tag{14}$$

$$\sigma_1=\frac{\bar{n}_e}{n_e}\frac{\lambda}{\bar{\lambda}} \tag{15}$$

$$\sigma_2=\frac{\bar{n}_e}{n_e}\sqrt{\frac{\bar{r}_{33}}{r_{33}}} \tag{16}$$

In what follows, we will find the modes of the waveguide, $\psi(\bar{s})$, in a waveguide induced by a gray photovoltaic soliton. First, let us solve Eq. (9) numerically for various values of ρ and find the soliton wave forms $\varphi(s)$. We then solve Eq. (12) for $\psi(\bar{s})$ by a numerical shooting method and transfer it to $\psi(s)$, so that both $\psi(s)$ and $\varphi(s)$ can be shown on the same plot. Note that the eigenvalue $\bar{\tau}$ must be in the range between $\delta(J-\rho)/(1+\rho)$ and $\delta(J-\rho m)/(1+\rho m)$ to fulfill the condition that the propagation constant of a guided mode, $\bar{\beta}$, lies between the maximum and the minimum values of the refractive index $\bar{n}_e(x)$ times the wave vector $\bar{k}_0$. To illustrate our results, let us consider the $LiNbO_3$ crystal with the following parameters $n_e=2.2$, $r_{33}=30\times10^{-12}$ m/V, and $E_p=40$ KV/cm. Let us also assume that $\lambda_0=0.5$ μm and $x_0=40$ μm. First, consider the various values of ρ that affect the soliton-induced waveguide. Fig. 1(a) shows the normalized field profiles of such gray photovoltaic solitons $\varphi(s)$ and the normalized field profiles of guided modes $\psi(s)$ for three different values of ρ when $J=1$, $m=0.2$, and $\sigma_1\sigma_2=0.735$. It reveals that the confined energy near the center of the gray photovoltaic soliton decreases with an increase in ρ. Second, consider the various values of m that affect the soliton-induced waveguide. Fig. 1(b) depicts the normalized field profiles of gray photovoltaic solitons $\varphi(s)$ and the normalized field profiles of guided modes $\psi(s)$ for three different values of m when $J=10$, $\rho=30$, and $\sigma_1\sigma_2=0.735$. Evidently, the confined energy near the center of the gray photovoltaic soliton decrease with an increase in m. Third, consider the various values of J that affect the soliton-induced waveguide. Fig. 2 depicts the normalized field profiles of such gray photovoltaic solitons $\varphi(s)$ and the normalized field profiles of guided modes $\psi(s)$ for three different values of J when $\rho=30$, $m=0.2$, and $\sigma_1\sigma_2=0.735$. As is clearly apparent from this figure, the confined energy near the center of the gray photovoltaic soliton increases with J. Moreover, Fig. 3 shows the number of guided modes and the propagation constants as a function of ρ at $m=0.2$, 0.5, and 0.8 when $J=0$ and $\sigma_1\sigma_2=0.735$. The number of guided modes at each ρ is given by the

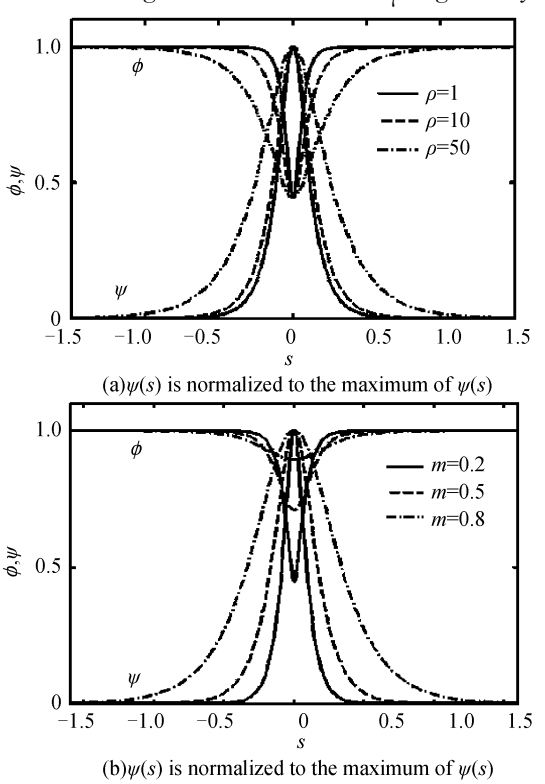

Fig. 1　Normalized field profiles of gray photovoltaic solitons and the normalized field profiles of guided modes for different ρ and m

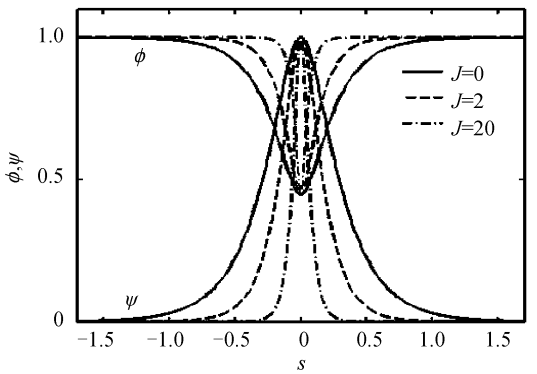

Fig. 2 Normalized field profiles of gray photovoltaic solitons and the normalized field profiles of guided modes for $J=0$, 2 and 20

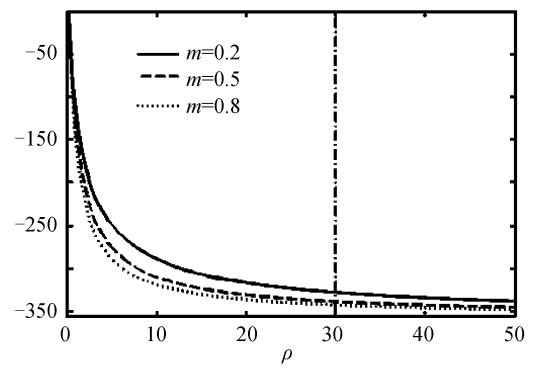

Fig. 3 Propagation constants of the guided modes of the waveguides induced by gray photovoltaic solitons

number of intersections of the dash-dot vertical line with the curves of the propagation constant in Fig. 3[14]. The dash-dot line corresponds to $\rho=30$ (the example given in Fig. 2). A close examination Figs. 1 ~ 3 indicates that waveguides induced by gray photovoltaic solitons are always single guided mode for both all soliton graynesses and all values of both ρ and J. Fig. 3 also shows that the propagation constant decreases with an increase in both ρ and m.

2 Conclusion

In conclusion, we have presented the theory of waveguides induced by gray solitons in closed-circuit photovoltaic crystals. We have found that waveguide induced by gray closed-circuit photovoltaic solitons are only a single guided mode for all values of the set of parameters m, ρ, and J. Our analysis indicates that the confined energy near the center of a gray closed-circuit photovoltaic soliton increases with J and decreases with an increase in both m and ρ.

References

[1] GUO Ru, LING Zhen-fang, CHEN Xiao-hu, *et al*. Saturable nonlinearity in photovoltaic- photorefractive crystals under open-circuit condition[J]. *Chin Phys Lett*, 2000, **17**(11): 804-805.

[2] HOU Chun-feng, PEI Yan-bo, ZHOU Zhong-xiang, *et al*. Bright-dark incoherently coupled photovoltaic soliton pair[J]. *Chin Phys*, 2005, **14**(2): 349-352.

[3] SHE Wei-long. Quantization of light energy directly from classical electromagnetic theory in vacuum[J]. *Chin Phys*, 2005, **14**(12): 2514-2521.

[4] MA Yang-hua, ZHANG Peng, ZHAO Jian-lin, *et al*. Numerical investigation of interactions among planar bright photorefractive screening solitons[J]. *Acta Photonica Sinica*, 2006, **35**(2): 252-256.

[5] SEGEV M, VALLEY G C, CROSIGNANI B, *et al*. Steady-state spatial screening solitons in photorefractive materials with external applied field[J]. *Phys Rev Lett*, 1994, **73**(24): 3211-3214.

[6] CHRISTODOULIDE D N, CARVALHO M I. Bright, dark, and gray spatial soliton states in photorefractive media[J]. *JOSA B*, 1995, **12**(9): 1628-1633.

[7] LI Jin-ping, LU Ke-qing, ZHAO Wei, *et al*. Experimental study on dark photovoltaic solitons[J]. *Acta Phonica Sinica*, 2006, **35**(8): 1125-1128.

[8] SEGEV M, VALLEY G C, BASHAW M C, *et al*. Photovoltaic spatial solitons[J]. *JOSA B*, 1997, **14**(7): 1772-1781.

[9] LU K Q, TANG T T, ZHANG Y P. One-dimensional steady-state spatial solitons in photovoltaic photorefractive materials with an external applied field[J]. *Phys Rev A*, 2000, **61**(5): 053822-053826.

[10] FAZIO E, RENZI F, RINALDI R, *et al*. Screening-photovoltaic bright solitons in lithium niobate and associated single-mode waveguides[J]. *Appl Phys Lett*, 2004, **85**(12): 2193-2195.

[11] LAN S, DELRE E, CHEN Z G, *et al*. Directional coupler with soliton-induced waveguides[J]. *Opt Lett*, 1999, **24**(7): 475-477.

[12] CHEN Z G, MITCHELL M and SEGEV M. Steady-state photorefractive soliton-induced Y-junction waveguides and high-order dark spatial solitons[J]. *Opt Lett*, 1996, **21**(10): 716-718.

[13] LAN S, SHIH M, MIZELL G, *et al*. Second-harmonic generation in waveguides induced by photorefractive spatial solitons[J]. *Opt Lett*, 1999, **24**(16): 1145-1147.

[14] SHIH M F, CHEN Z G, MIZELL M, *et al*. *VWaveguides induced by photorefractive screening solitons*[J]. JOSA B, 1997, **14**(11): 3091-3101.

[15] *TAYA M, BASHAW M, FEJER M M*, et al. *Observation of dark photovoltaic spatial solitons*[J]. Phys Rev A, 1995, **52**(4): 3095-3100.

[16] *LU K Q, ZHAO W, YANG Y L*, et al. *Soliton-induced waveguides in photorefractive photovoltaic materials*[J]. J Mod Optic, 2006, **53**(15): 2137-2151.

[17] *LU Ke-qing, ZHANG Mei-zhi, ZHAO Wei*, et al *Waveguides induced by screening-photovoltaic solitons in biased photorefractive-photovoltaic crystals*[J]. Chin Phys Lett, 2006, **23**(10): 2770-2773

闭路光伏灰孤子诱导的波导

陈丹[1]，张美志[2,3]，杨延龙[3]，卢克清[3]
(1 西安电子科技大学 综合业务网理论及关键技术国家重点实验室，西安 710071)
(2 西安邮电学院电子工程学院，西安 710061)
(2 中国科学院西安光学精密机械研究所 瞬态光学与光子技术国家重点实验室，西安 710119)

摘　要：理论分析了闭路光伏晶体中灰孤子诱导的波导. 研究发现，闭路光伏灰孤子诱导的波导在不同孤子灰度值，电流密度和光强比率下均为单模，文中光强比率指孤子峰值强度与暗辐射之比. 研究结果解释了闭路光伏灰孤子限制在中心的能量随着电流密度的增加而增加，随着孤子灰度值和光强比率的增加而减小. 文章还提供了光伏晶体的相关例子.

关键词：孤子波导；光折变效应；非线性光学

CHEN Dan　was born in 1984. He received the B. S. degree from School of Telecommunication Engineering, Xidian University in 2006. Now he is a Ph. D. candidate at Xidian University, and his research interests focus on ad hoc networks and optical communication.